INVITED PAPER Special Section on Extremely Advanced Optical Transmission Technologies and Transmission Optical Fiber Technologies towards Exabit Era

Ultra-High Capacity Optical Transmission Technologies for 100 Tbit/s Optical Transport Networks

Akihide SANO†a), Takayuki KOBAYASHI†, Eiji YOSHIDA†, *Members*, *and* Yutaka MIYAMOTO†, *Fellow*

SUMMARY This paper describes ultra-high capacity wavelength-division multiplexed (WDM) transmission technologies for 100-Tbit/s-class optical transport networks (OTNs). First, we review recent advances in ultra-high capacity transmission technologies focusing on spectrally-efficient multi-level modulation techniques and ultra-wideband optical amplification techniques. Next, we describe an ultra-high capacity WDM transmission experiment, in which high speed polarization-division multiplexed (PDM) 16-ary quadrature amplitude modulation (16-QAM), generated by an optical synthesis technique, in combination with coherent detection based on digital signal processing with pilotless algorithms, realize the high spectral efficiency (SE) of 6.4 b/s/Hz. Furthermore, ultra-wideband hybrid optical amplification utilizing distributed Raman amplification (DRA) and C- and extended L-band erbium-doped fiber amplifiers (EDFAs) is shown to realize 10.8-THz total signal bandwidth. By using these techniques, 69.1-Tbit/s transmission is demonstrated over 240-km of pure silica-core fibers (PSCFs). Furthermore, we describe PDM 64-QAM transmission over 160 km of PSCFs with the SE of 9.0 b/s/Hz.
key words: *coherent optical communication, multi-level modulation, QAM, Raman amplification*

1. Introduction

Driven by the increasing demand for novel broadband services such as video-sharing, high-definition video-on-demand, and network computing, Internet traffic has been increasing steadily at the rate of about 40% per year. To support this flood of data traffic, the carriers' backbone networks must be based on high-capacity optical transport networks (OTNs) [1]. Wavelength-division multiplexed (WDM) systems based on wideband erbium-doped fiber amplifiers (EDFAs) have drastically reduced transport cost in backbone OTNs. Conventional C- and L-band EDFAs offer the gain bandwidth of 4 THz, and the total capacity of WDM systems has been extended by increasing the spectral efficiency (SE) by reducing the channel spacing and increasing the channel rate. The channel rate of commercial WDM systems using on-off keying (OOK) and direct detection increased from 2.5 to 10 Gbit/s/ch, and 40-Gbit/s/ch interfaces have been already deployed in backbone OTNs [2] by employing phase-shift keying modulation and differential direct detection such as differential quadrature phase-shift keying (DQPSK) [3].

Since the higher-speed local area network (LAN) interfaces of 100 Gbit/s Ethernet have been standardized recently, there are emerging demands for the long-haul transport of 100-Gbit/s channels over OTNs [4]. Polarization-division multiplexed (PDM) QPSK with intradyne coherent reception is very promising for the long-haul transmission of 100-Gbit/s channels [5]. The powerful equalization capabilities provided by digital signal processing (DSP) effectively eliminates the signal distortion caused by chromatic dispersion (CD) and polarization-mode dispersion (PMD) that are the main factors limiting the attainable distance of high-speed transmission. Furthermore, PDM is effective in improving the SE, and thus 50-GHz channel spacing (2 bit/s/Hz) will be feasible. This means that total capacities of about 8 (C- or L-band) to 16 Tbit/s (C- and L-band) can be expected.

In future OTNs, further advances are indispensable in terms of both SE and total signal bandwidth in order to handle the unstoppable increase in data traffic. In this paper, we describe ultra-high capacity optical transmission technologies to realize 100-Tbit/s-class total capacity. Section 2 reviews the evolution of high capacity optical transmission technologies in terms of the SE and bandwidth of optical amplifiers. In Sect. 3, we describe a 69.1-Tbit/s ultra-high capacity WDM transmission experiment that utilizes spectrally-efficient PDM 16-ary quadrature amplitude modulation (QAM) and ultra wideband hybrid amplification of C- and extended L- (L^+-) band EDFAs and distributed Raman amplification (DRA). Section 4 focuses on higher SE multi-level transmission based on PDM 64-QAM modulation to achieve the SE of 9 b/s/Hz. Section 5 summarizes our conclusions.

2. Large Capacity Transmission Technologies

Figure 1 shows the evolution of the total capacity per single fiber as demonstrated by laboratory transmission experiments reported as postdeadline papers in major conferences such as OFC and ECOC. Earlier trials, before 2002, employed binary OOK modulation and direct detection, in which the SE was improved by increasing the bit rate; 10.92-Tbit/s transmission was attained by using the 40-Gbit/s/ch non-return-to-zero (NRZ) OOK format with the SE of 0.8 b/s/Hz and triple band optical fiber amplifiers in the S-, C-, and L-bands with the total signal bandwidth of 13.65 THz [6], and 10.2-Tbit/s transmission was demonstrated by using the vestigial side-band (VSB) and polarization-multiplexing technique with the SE of 1.28 b/s/Hz in C- and L-bands [7].

Manuscript received November 23, 2010.
Manuscript revised November 29, 2010.
†The authors are with NTT Network Innovation Laboratories, NTT Corporation, Yokosuka-shi, 239-0847 Japan.
a) E-mail: sano.akihide@lab.ntt.co.jp
DOI: 10.1587/transcom.E94.B.400

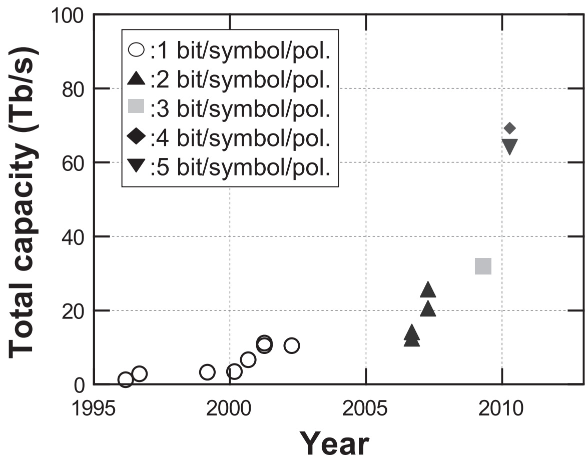

Fig. 1 Evolution of total capacity per fiber.

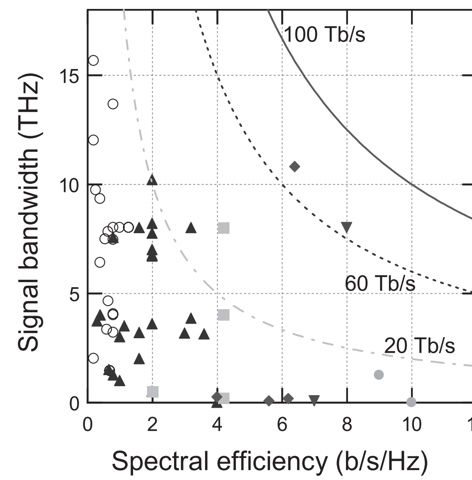

Fig. 2 Spectral efficiency and Total signal bandwidth of recent transmission experiments. ○: 1 bit/symbol/pol., ▲: 2 bit/symbol/pol., ■: 3 bit/symbol/pol., ♦: 4 bit/symbol/pol., ▼: 5 bit/symbol/pol., ●: ≥6 bit/symbol/pol.

In the next generation, further capacity extension was enabled by employing the DQPSK format to double the SE; 25.6-Tbit/s transmission was demonstrated by using 85.6 Gbit/s/ch PDM return-to-zero (RZ) DQPSK with the SE of 3.2 b/s/Hz and 8-THz total signal bandwidth in C- and L-bands [8], and 20.4-Tbit/s transmission was demonstrated by using 111-Gbit/s/ch carrier-suppressed RZ (CSRZ) DQPSK with the SE of 2 b/s/Hz and 10.2-THz seamless signal bandwidth in C- and L^+-bands [9].

Recent developments in coherent detection technology based on DSPs have enabled further enhancement of SE in combination with multi-level modulation and PDM. 32-Tbit/s transmission was demonstrated by using 114-Gbit/s/ch PDM RZ 8-ary quadrature amplitude modulation (8-QAM) with the SE of 4 b/s/Hz and 8-THz C- and L-band optical amplification [10]. Recently, 64-Tbit/s transmission was demonstrated by using PDM 36-QAM modulation with the SE of 8 b/s/Hz and C- and L-band optical amplification [11]. Moreover, the highest capacity of 69.1-Tbit/s was realized by using PDM 16-QAM modulation with the SE of 6.4 b/s/Hz and 10.8 THz ultra-wideband hybrid amplification in C- and L^+-bands [12] as is described in Sect. 3.

Figure 2 plots the SE and signal bandwidth of recent high-capacity and/or high-SE transmission experiments. Total capacity is given by the product of SE and signal bandwidth, and the contour curves of 20, 60, and 100 Tbit/s total capacities are also shown. The orders of the multi-levels are represented by different symbols. As shown in Fig. 2, multi-level modulation is indispensable to increase the SE. The highest SE of 10 b/s/Hz was demonstrated by using 14 Gbit/s PDM 128-QAM signal (1 Gbaud) with 1.4-GHz channel spacing [13]. In 100-Gbit/s/ch-class transmission, 9 b/s/Hz was realized by using 120-Gbit/s/ch PDM 64-QAM modulation with 12.5-GHz channel spacing [14] as is described in Sect. 4. It should be noted that higher order multi-level formats are susceptible to both amplitude and phase noise due to their tight constellations. Therefore, low-loss and low-nonlinearity transmission lines as well as low-noise optical amplification techniques such as DRA are indispensable to suppress the optical signal-to-noise (OSNR) degradation and nonlinear-induced distortion and phase noise. Dense wavelength-multiplexing/demultiplexing techniques are also important to obtain high SE values. Narrow-band signal generation utilizing digital filters and digital-to-analog converters (DACs) were demonstrated to reduce the crosstalk from adjacent channels [11], [13] at the baud rate below 10.7 Gbaud. In higher baud rate systems, optical filtering techniques have been employed [15], [16], and the SE of 4 b/s/Hz was realized in 28-Gbaud PDM QPSK transmission with the aid of maximum a posteriori (MAP) detection [15].

Wideband optical amplification is also indispensable to achieve 100-Tbit/s total capacity. Current commercial EDFAs have the gain bandwidths of about 4 THz for C- and L-bands each, so most of the reported transmission experiments were demonstrated with the signal bandwidth below 8 THz. In this case, however, SE should be higher than 12.5 b/s/Hz in order to realize the total capacity of 100 Tbit/s. This requires the use of higher order multi-level modulation with 128 or 256 levels, and thus very sophisticated transmitter/receivers and transmission lines are required. DRA is very promising to extend the total signal bandwidth to over 8 THz. Most of the over-10-THz-class transmission experiments employed DRA techniques. 12.5-THz seamless signal bandwidth was obtained by using all-Raman amplification [17], and 15.5 THz signal bandwidth was realized by tellurite/silica fiber Raman amplification techniques [18]. The use of these wideband amplification techniques will alleviate the requirements imposed by the use of higher order multi-level format.

3. 69.1-Tbit/s PDM-16-QAM Transmission Experiment

High SE modulation/multiplexing and ultra-wideband op-

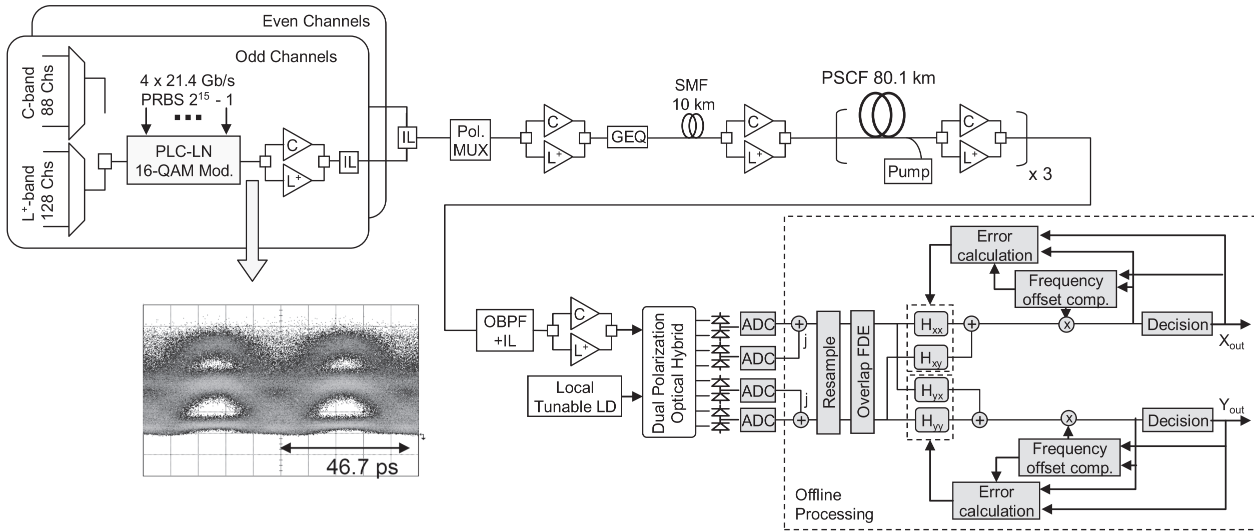

Fig. 3 Experimental setup of 69.1-Tbit/s PDM 16-QAM transmission experiments.

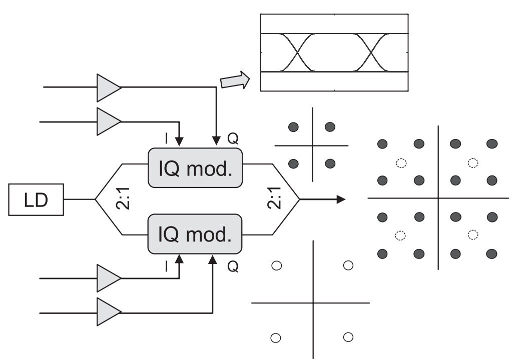

Fig. 4 Optical synthesis of a 16-QAM signal.

tical amplification techniques are indispensable to extend the total capacity. In this section, we describe an ultra-high capacity PDM 16-QAM transmission experiment based on these techniques. The total capacity of 69.1 Tbit/s is the highest ever reported for a single fiber.

Figure 3 shows the entire experimental setup, and the 16-QAM signal generation scheme is shown in Fig. 4. We employed a signal synthesis scheme in the optical domain [19]–[22]. As shown in Fig. 4, the modulator consists of two IQ modulators (IQMs) in parallel configuration, an optical splitter, and a combiner, where each IQM is driven by a pair of binary electrical signals to output a QPSK signal. QPSK signals from the two IQMs are coupled with an amplitude ratio of 2:1 to form a 16-QAM signal. In this configuration, since each IQM is driven by electrical binary signals, high linearity is not required from each driver amplifier. Thus high-speed operation can be expected. Moreover, thanks to the transmission characteristics of each MZM, inter-symbol interference (ISI) suppression can be expected [19]. Thus this approach is promising for high speed QAM signal generation. The modulator was fabricated by utilizing the hybrid integration technology of silica planar lightwave circuits (PLCs) and $LiNbO_3$ phase modulator arrays [23]. The loss of the modulator was about 6.4 dB, and electro-optical (EO) 3-dB bandwidth was larger than 25 GHz, which is sufficient for 21.4-Gbaud operation. Furthermore, by employing this PLC-LN platform and using the tri-parallel IQM configuration, 64-QAM signal generation was achieved [21], and a 20-Gbaud PDM 64-QAM signal (240 Gbit/s) was successfully generated and demodulated [22].

We utilized this 16-QAM signal generation scheme to confirm ultra-high capacity transmission performances. At the transmitter, as shown in Fig. 3, 432 CW optical carriers (1527.22–1562.03, and 1565.91–1619.84 nm) with a 25-GHz spacing in C- and L^+-bands were generated. The odd/even channels were separately multiplexed, and modulated to create 21.4 Gbaud 16-QAM signals. Due to the narrow linewidth requirement of 16-QAM [24], we used a tunable external-cavity laser (ECL) or a narrow-linewidth L-band tunable DFB laser array (TLA) [25] as the signal light source under test; the linewidths of the ECL and the TLA were about 100–200 kHz. The remaining light sources were DFB-LDs with linewidths of several MHz. Two sets of 85.6-Gbit/s 16-QAM signals with 50-GHz spacing were generated. We employed a dual-stage interleaver (IL) to combine even and odd signals with 25-GHz spacing to suppress inter-channel crosstalk, and polarization-multiplexed them to form 171.2-Gbit/s PDM 16-QAM signals in a polarization multiplexer with a 10-ns delay line. A 10-km single-mode fiber (SMF) for signal decorrelation was inserted before the transmission line (This only had minor impacts because of large local dispersion of the transmission line). Figure 5 shows the optical spectra for even and odd channels after passing through a two-stage IL. The 20-dB down spectral width after the dual-stage IL was about 27 GHz. We can confirm that the signal powers of adjacent channels are suppressed to less than 45 dB at the center frequency of the 25-GHz grid. The line rate was 171.2 Gbit/s, and after subtracting 7% FEC overhead, the data rate was 160 Gbit/s, and

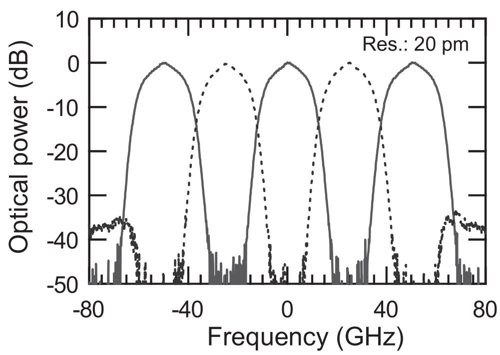

Fig. 5 Optical spectra of 25-GHz spaced 171-Gbit/s PDM 16-QAM signals.

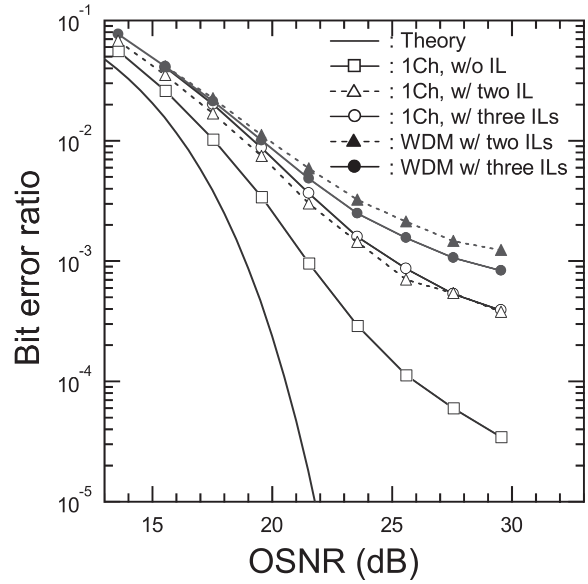

Fig. 6 Back-to-back bit error rate characteristics of 171-Gbit/s PDM 16-QAM signals.

the SE was 6.4 b/s/Hz, the highest yet reported for 16-QAM transmission.

The transmission line consisted of three 80.1-km spans of low-loss and low-nonlinear pure silica core fiber (PSCF) [26], [27] and three in-line dual-band EDFAs. The loss coefficient of PSCF and the loss of an 80.1-km span were 0.160 dB/km and 13.5 dB at 1570 nm, respectively. The effective area, the average value over the three spans, was 110 μm^2. The dispersion and dispersion-slope were 21.8 ps/nm/km and 0.056 ps/nm^2/km at the wavelength of 1575 nm, respectively. The dual-band EDFA incorporated a C-band EDFA, an L^+ -band EDFA [28], and gain-flattening filters for DRA (GFF-R), where both EDFAs employed dual-stage amplification with an intermediate GFF (GFF-E) so as to achieve low noise-figures (NF) and high output powers. Backward-pumped DRAs with pump wavelengths of 1430, 1440, 1470, 1490, and 1505 nm were used to improve the optical signal-to-noise ratio (OSNR) of the transmitted signal. The average signal power launched into PSCF was about −5 dBm/ch.

At the receiver side, the received signals were demultiplexed by a 25/50 GHz IL and optical bandpass filters, and then detected by the polarization-diversity intradyne receiver. The received signal was mixed with a CW light from a free-running local oscillator (LO) in a PLC-based dual polarization optical hybrid (DPOH) [29] which contained two sets of polarization beam splitter (PBS) and 90 degree optical hybrid. The linewidth of the LO was ~100 kHz. The carrier frequency offset between the LO and the transmitted light source was tuned to within 20 MHz. The real and imaginary components of the two polarizations were detected by balanced photo-diodes, amplified by broadband electrical amplifiers, digitized at 50-GSamples/s, and stored in sets of 1M samples by using a digital storage oscilloscope with a 20-GHz analog bandwidth. These data were post-processed off-line.

The offline-processing structure is also shown in Fig. 3 [30]. After re-sampling to 2 Samples/Symbol (42.8 GS/s), CD of the entire transmission line was fully digitally compensated by utilizing fixed-tap overlap frequency domain equalization (FDE) [31]. Polarization demultiplexing and signal equalization were conducted by 27-tap T/2-spaced adaptive FIR filters in the butterfly configuration. In the first stage of equalization, the tap coefficients were optimized under the control of the pilotless algorithm based on the constant modulus algorithm- (CMA-) multimodulus algorithm (MMA) [32]. It took about 1.3 μs for this pre-convergence. MMA can recover carrier phase offset automatically but is weak against carrier frequency offset. Therefore, we also employed a frequency offset compensator based on a digital phase lock loop (PLL) [33]. After pre-convergence, the adaptive filter tap control algorithm was switched from CMA-MMA to decision-directed least mean squares (LMS) algorithm [34]. Finally, bit error ratio (BER) was calculated from the 1.8 Mbit demodulated signal.

Figure 6 shows the measured BER performance of 171.2 Gbit/s PDM 16-QAM signals as a function of OSNR in the back-to-back configuration. The measured wavelength was 1552.52 nm. The squares plot the single-channel measurements without using IL; the OSNR (0.1-nm resolution) required to obtain a BER of 1×10^{-3} was 21.5 dB. This value is 2.7 dB off the theoretical limit for PDM 16-QAM. Open triangles and circles show the results for the single-channel case with two (single IL for both Tx and Rx side) and three (dual-stage IL at Tx and single IL at Rx) ILs, respectively. The OSNR penalties are about 3.6 dB, and no significant differences are observed. In the 25-GHz spaced 5-channel WDM case (filled triangles and circles), two-IL case (filled triangles) exhibits degradation in the low BER region due to crosstalk from adjacent channels. In the three-IL case, however, we can confirm that better BER performance under 1×10^{-3} is possible in spite of the additional penalty of 2.8 dB. Based on these results, we employed the dual-stage IL configuration at the Tx. Figure 7(a) shows the constellation diagrams for both polarizations in the single-channel PDM case without ILs at the OSNR of 30 dB. We

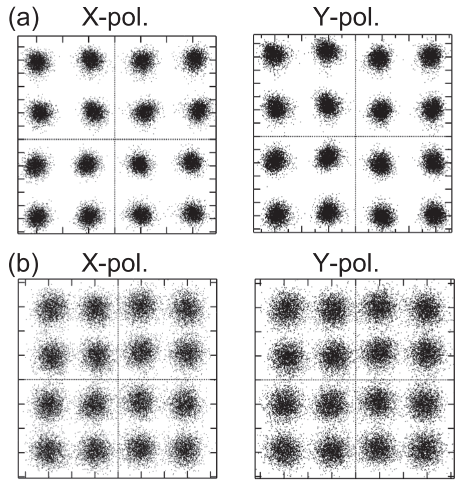

Fig. 7 Constellation diagrams of 171-Gbit/s PDM 16-QAM signals. (a) Back-to-back. (b) After 240-km transmission.

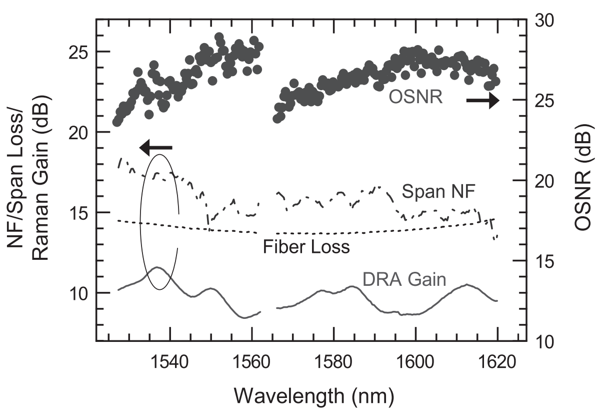

Fig. 8 Spectra of received OSNR, span NF, fiber loss, and DRA gain.

can confirm clear constellation for both polarizations, which demonstrates the successful operation of signal demodulation and equalization.

Next, we discuss the performance of the ultra-wideband hybrid Raman/EDFA amplification arrangement. Figure 8 shows the spectra of the span loss, DRA gain, and span NF of a single span (the first 80.1-km span), and the received OSNR after 240-km transmission. The DRA gain includes the pump-signal and signal-signal stimulated Raman scattering (SRS), and ranged from 8.4 to 11.6 dB. The span NF ranged from 13.1 to 18.4 dB, which tends to decrease as the signal wavelength increases. The received OSNR ranged from 23.6 to 28.9 dB in the C-band, and from 23.8 to 28.1 dB in the L^+-band.

The received signal spectra (20-pm resolution) are shown in Fig. 9; the signal bandwidths for C- and L^+-bands are 4.4 and 6.4 THz, respectively. The measured BER performance of all 432 channels after 240-km transmission is also shown in Fig. 9. In both bands, shorter wavelength channels have lower Q-factors, which reflect the received OSNR characteristics. Taking account of the measured OSNR tolerance in the back-to-back WDM case, received

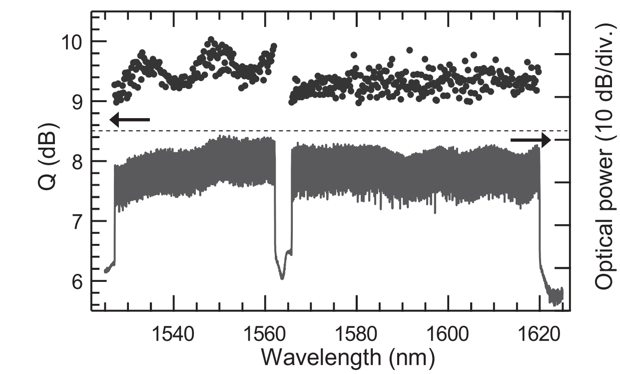

Fig. 9 Spectra of Q-factors and received signals in 69.1-Tbit/s 240-km transmission.

BER performance was mainly determined by OSNR performance thanks to the low fiber input power of −5 dBm/ch and the large effective area of the PSCFs. In addition, Q-factor fluctuation in L^+-band is slightly larger than that in C-band. We attribute this to deviation in the orthogonality of the DPOH, which was designed for C-band use. We confirmed that the Q-factors of all 432 channels were better than 9.0 dB, which exceeds the Q-limit of 8.5 dB (dashed line) yielding BERs below 1×10^{-12} with the use of today's commercial 10-Gbit/s FEC techniques with 7% overhead [35]. The constellation diagrams of a 1527.99-nm channel after 240-km transmission, shown in Fig. 7(b), confirm the maintenance of a clear constellation.

4. 11.2-Tbit/s 64-QAM Transmission Experiments

In order to increase SE further, higher order multi-level modulation is attractive. In this section, we discuss the high SE transmission performance of PDM 64-QAM modulation that can carry 12 bits/symbol.

The signal generation scheme used here is shown in Fig. 10. Unlike the 16-QAM transmission described in Sect. 3, we employed a single IQM driven by electrical multi-level signals generated by DACs. This is a versatile configuration for arbitrary optical waveform generation, and supports a wide variety of modulation formats. The modulation speed is, however, limited by DAC sampling rate; the symbol rate was 10.03 Gbaud with 1 sample/symbol operation. The vertical resolution of DACs was 8 bits. As shown in Fig. 10, we used two electrical 8-level signals to obtain 64-QAM signals in this experiment.

Figure 11 shows the setup for PDM 64-QAM WDM transmission. We employed two transmitters for the even and for the odd channels. The even-channel transmitter used 25 CW lasers with carrier frequencies on the ITU-T 50-GHz grid. The 25 optical carriers were multiplexed, and simultaneously modulated by an LN IQM driven by two 10.03-Gbaud 8-level electrical signals with the pattern length of $2^{15} - 1$ symbols. The driving amplitude of the IQM was about 25% of the full-swing voltage so as to operate the modulator in the linear condition. The higher frequency components of the modulated signals were filtered

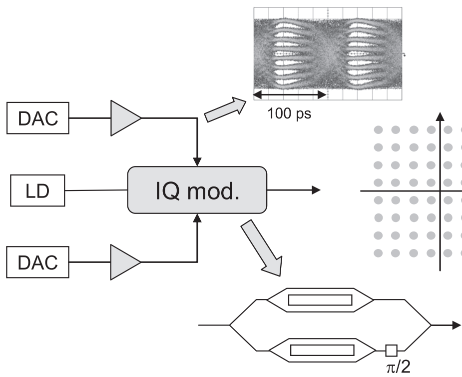

Fig. 10 Signal generation of 64-QAM signal using digital-to-analog converters.

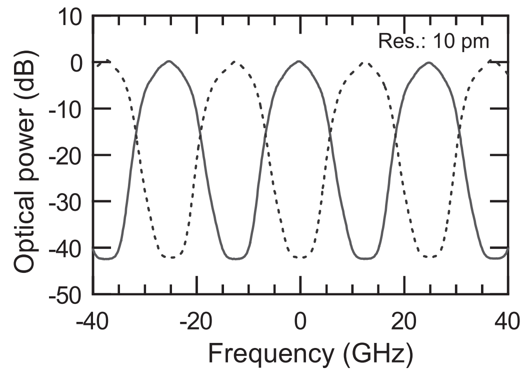

Fig. 12 Optical spectra of 12.5-GHz spaced 120-Gb/s/ch PDM 64-QAM signals.

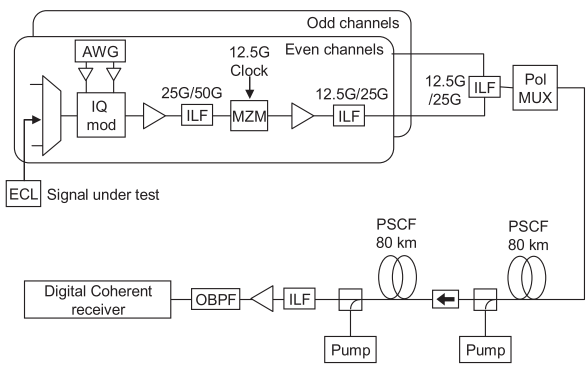

Fig. 11 Experimental setup of 120 Gbit/s/ch PDM 64-QAM signal transmission.

by a 50/25 GHz optical interleaving filter (ILF), and then modulated by an MZ modulator (MZM) driven by a 12.5-GHz clock and biased at the null point [36]. This converted the 50-GHz spaced 25-channel signals into 25-GHz spaced 50-channel signals; higher frequency components located at ±37.5 GHz away were suppressed below 40 dB to avoid inter-channel crosstalk [11]. The 25-GHz spaced signals were passed through a 25/12.5 GHz ILF to suppress inter-channel crosstalk. The odd-channel transmitter contained 25 CW lasers with frequencies shifted by 12.5 GHz from the ITU-T 50-GHz grid, and the signals were generated in the same manner as the even channels. Even and odd channels were multiplexed in an ILF to yield 12.5-GHz spacing, and polarization-multiplexed by splitting the signals, delaying one stream by ~100 symbols, and coupling the two streams in a polarization beam combiner. Consequently we obtained 100-channel 120.4 Gbit/s PDM 64-QAM signals with 12.5-GHz channel spacing. The decorelation of WDM channels was not performed in this experiment because WDM signals were rapidly decorelated in the transmission fiber due to its large local dispersion. After subtracting 7% FEC overhead, the data rate was 112.5 Gbit/s, and the SE was 9.0 b/s/Hz. As shown in Fig. 11, we used a tunable ECL with a linewidth of about 60 kHz as the light source for the signal under test, and the remaining lasers were DFB-LDs (linewidth ~2 MHz). The optical spectra for even and odd channels after the ILFs are shown in Fig. 12.

The transmission line consisted of two 80.1-km spans of low-loss and low-nonlinear PSCF, the same fiber used in 16-QAM transmission described in Sect. 3. In order to cope with the increase in required ONSR, we utilized all-Raman amplification; the backward-pumped distributed Raman amplifiers (DRA) with pump wavelengths from 1430 to 1490 nm yielded the on-off gain of 16 dB. The fiber input power was −12 dBm/ch.

The received signals were demultiplexed by an ILF and optical bandpass filters (OBPF), and detected by a polarization-diversity intradyne receiver containing a PLC-based DPOH [29] with high accuracy in 90-degree phase difference. We used a free-running ECL with a linewidth of ~70 kHz as the LO. The frequency offset between the LO and the received signal was tuned to within 20 MHz. Real and imaginary parts of the two polarization tributaries were detected by four balanced photo detectors, digitized at 50 GS/s using a digital storage oscilloscope, and stored in sets of 2M samples. These data were post-processed off-line.

The configuration of the offline signal processing is almost same as that in Sect. 3, but IQ imbalance (both amplitude and phase) was digitally compensated by utilizing a pilotless estimation algorithm in conjugate signal models [37].

Figure 13 shows the measured BER performance as a function of OSNR in the back-to-back configuration. The circles represent the measured values of single-channel PDM 64-QAM without using ILFs; the required OSNR (0.1-nm resolution) to obtain the BER of 1×10^{-3} was 27.1 dB. This value is 5.6 dB off the theoretical limit. The constellation diagrams at the OSNR of 36.5 dB are shown in Fig. 14(a). After passing through ILFs (triangles), an excess ONSR penalty of 1.8 dB was observed due to tight optical filtering. In the 12.5-GHz spaced WDM case (squares), although an additional penalty of 2.0 dB was incurred due to the crosstalk from neighbouring channels, we confirmed that BERs under 1×10^{-3} are possible.

Figure 15 shows the received optical spectra after 160-km transmission (10-pm resolution). The received OSNR

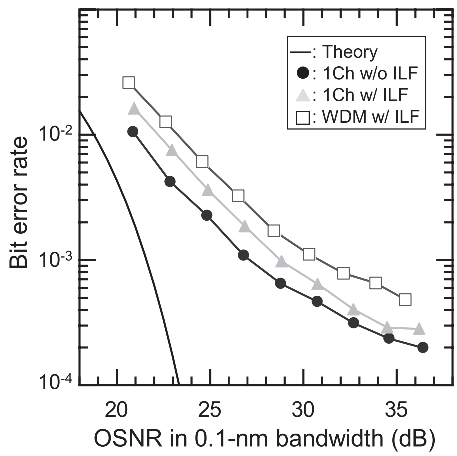

Fig. 13 Back-to-back bit error rate characteristics of 120-Gbit/s/ch PDM 64-QAM signals.

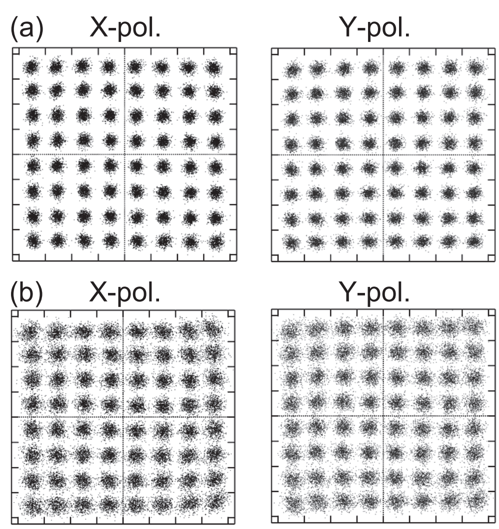

Fig. 14 Constellation diagrams of 120-Gbit/s/ch PDM 64-QAM signals. (a) Back-to-back. (b) After 160-km transmission.

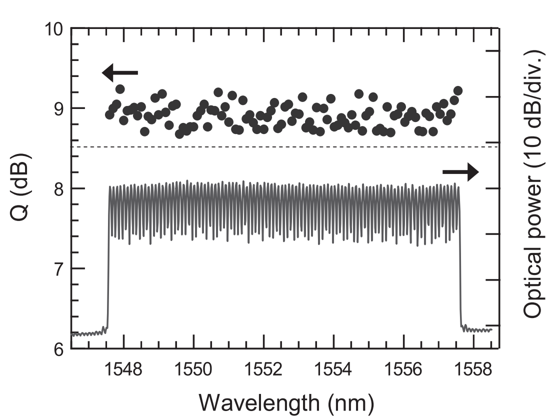

Fig. 15 Spectra of Q-factors and received optical signals of 11.2-Tbit/s 160-km transmission.

values were around 28 dB. The OSNR improvement over typical Raman/EDFA hybrid amplification is estimated to be ∼1.5 dB. Measured Q factors after 160-km transmission are also shown in Fig. 15. The Q-factors of all 100 channels were confirmed to be better than 8.7 dB with the average value of 8.9 dB, which exceed the Q-limit of 8.5 dB (dashed line) yielding BERs below 1×10^{-12}.

5. Conclusion

In this paper, we described ultra-high capacity WDM technologies toward 100-Tbit/s-class total capacity. Both high SE and wideband optical amplification are essential to realize such high capacity systems. Multi-level modulation formats like 16-QAM or 64-QAM are very promising to improve the SE. In addition, higher order multi-level transmission necessitates the use of low-loss and low-nonlinearity transmission lines as well as low-noise optical amplification techniques such as DRA in order to suppress OSNR degradation and nonlinear-induced distortion and phase noise. Raman amplification is also attractive to realize 10-THz-class signal bandwidth.

Next, we described an ultra-high capacity WDM transmission experiment using PDM 16-QAM modulation. The high speed 21.4-Gbaud PDM 16-QAM signals were generated by an optical synthesis technique and detected by a coherent receiver based on DSP with pilotless algorithms, and the SE of 6.4 b/s/Hz was achieved, the highest yet reported for 16-QAM transmission. Ultra-wideband hybrid optical amplification utilizing DRA and C- and L^+-band EDFAs realized 10.8-THz total signal bandwidth. By using these techniques, 69.1-Tbit/s transmission was demonstrated over 240-km of PSCF.

We also described 11.2-Tbit/s PDM 64-QAM transmission over 160 km of PSCFs. The SE was 9.0 b/s/Hz, which is the highest yet reported for 100-Gbit/s/ch-class transmission.

Acknowledgments

The authors thank K. Hagimoto, T. Nakashima, Y. Hibino, T. Enoki, S. Matsuoka, K. Okada, S. Suzuki, H. Oohashi, and H. Hadama for their continuous encouragement. The authors also thank their colleagues in NTT Laboratories for fruitful discussions and technical support.

References

[1] Y. Miyamoto and S. Suzuki, "Advanced optical modulation and multiplexing technologies for high-capacity OTN based on 100 Gb/s channel and beyond," IEEE Commun. Mag., vol.48, no.3, pp.S65–S72, March 2010.

[2] T. Kataoka, S. Matsuoka, T. Matsuda, H. Maeda, N. Sakaida, T. Kubo, T. Kotanigawa, and T. Kawasaki, "Field transmission by using a commercially-ready 43 Gbit/s DWDM system employing RZ-DQPSK transponders in high PMD installed fiber," Proc. OFC/NFOEC2007, paper JThA45, March 2007.

[3] R.A. Griffin and A.C. Carter, "Optical differential quadrature phase-shift key (oDQPSK) for high capacity optical transmission," Proc.

OFC2002, paper WX6, March 2002.
[4] J. Roese, R.-P. Braun, M. Tomizawa, and O. Ishida, "Optical transport network evolving with 100 Gigabit Ethernet," IEEE Commun. Mag., vol.48, no.3, pp.S28–S34, March 2010.
[5] C.R.S. Fludger, T. Duthel, D. van den Borne, C. Schulien, E.-D. Schmidt, T. Wuth, J. Geyer, E. De Man, G.D. Khoe, and H. deWaardt, "Coherent equalization and POLMUX-RZ-DQPSK for robust 100-GE transmission," J. Lightwave Technol., vol.26, no.1, pp.64–72, Jan. 2008.
[6] K. Fukuchi, T. Kasamatsu, M. Morie, R. Ohhira, T. Ito, K. Sekiya, D. Ogasawara, and T. Ono, "10.92-Tb/s (273 × 40-Gb/s) triple-band/ultra-dense WDM optical-repeatered transmission experiment," Proc. OFC2001, paper PD24, March 2001.
[7] Y. Frignac, G. Charlet, W. Idler, R. Dischler, P. Tran, S. Lanne, S. Borne, C. Martinelli, G. Veith, A. Jourdan, J-P. Hamaide, and S. Bigo, "Transmission of 256 wavelength-division and polarization-division-multiplexed channels at 42.7 Gb/s (10.2 Tb/s capacity) over 3×100 km of TeraLight fiber," Proc. OFC2002, paper FC5-1, March 2002.
[8] A.H. Gnauck, G. Charlet, P. Tran, P.J. Winzer, C.R. Doerr, J.C. Centanni, E.C. Burrows, T. Kawanishi, T. Sakamoto, and K. Higuma, "25.6-Tb/s C+L band transmission of polarization-multiplexed RZ-DQPSK signals," Proc. OFC/NFOEC2007, paper PD19, March 2007.
[9] H. Masuda, A. Sano, T. Kobayashi, E. Yoshida, Y. Miyamoto, Y. Hibino, K. Hagimoto, T. Yamada, T. Furuta, and H. Fukuyama, "20.4-Tb/s (204 × 111 Gb/s) transmission over 240 km using bandwidth-maximized hybrid Raman/EDFAs," Proc. OFC/NFOEC2007, paper PD20, March 2007.
[10] X. Zhou, J. Yu, M.-F. Huang, Y. Shao, T. Wang, P. Magill, M. Cvijetic, L. Nelson, M. Birk, G. Zhang, S. Ten, H.B. Matthew, and S.K. Mishra, "Transmission of 32-Tb/s capacity over 580 km using RZ-shaped PDM-8QAM modulation format and cascaded multimodulus blind equalization algorithm," J. Lightwave Technol., vol.28, no.4, pp.456–464, Feb. 2010.
[11] X. Zhou, J. Yu, M.-F. Huang, Y. Shao, T. Wang, L. Nelson, P. Magill, M. Birk, P.I. Borel, D.W. Peckham, and R. Lingle, Jr., "64-Tb/s (640×107-Gb/s) PDM-36QAM transmission over 320 km using both pre- and post-transmission digital equalization," Proc. OFC/NFOEC2010, paper PDPB9, March 2010.
[12] A. Sano, H. Masuda, T. Kobayashi, M. Fujiwara, K. Horikoshi, E. Yoshida, Y. Miyamoto, M. Matsui, M. Mizoguchi, H. Yamazaki, Y. Sakamaki, and H. Ishii, "69.1-Tb/s (432 × 171-Gb/s) C- and extended L-band transmission over 240 km using PDM-16-QAM modulation and digital coherent detection," Proc. OFC/NFOEC2010, paper PDPB7, March 2010.
[13] M. Nakazawa, "Challenges to FDM-QAM coherent transmission with ultrahigh spectral efficiency," Proc. ECOC2008, paper Tu.1.E.1, Sept. 2008.
[14] A. Sano, T. Kobayashi, A. Matsuura, S. Yamamoto, S. Yamanaka, E. Yoshida, Y. Miyamoto, M. Matsui, M. Mizoguchi, and T. Mizuno, "100 × 120-Gb/s PDM 64-QAM transmission over 160 km using linewidth-tolerant pilotless digital coherent detection," Proc. ECOC2010, paper PD2.4, Sept. 2010.
[15] J.-X. Cai, Y. Cai, C.R. Davidson, D.G. Foursa, A. Lucero, O. Sinkin, W. Patterson, A. Pilipenskii, G. Mohs, and N.S. Bergano, "Transmission of 96×100G pre-filtered PDM-RZ-QPSK channels with 300% spectral efficiency over 10,608 km and 400% spectral efficiency over 4,368 km," Proc. OFC/NFOEC2010, paper PDPB10, March 2010.
[16] E. Torrengo, R. Cigliutti, G. Bosco, G. Gavioli, A. Alaimo, A. Carena, V. Curri, F. Forghieri, S. Piciaccia, M. Belmonte, A. Brinciotti, A. La Porta, S. Abrate, and P. Poggiolini, "Transoceanic PM-QPSK terabit superchannel transmission experiments at baud-rate subcarrier spacing," Proc. ECOC2010, paperWe7.C.2, Sept. 2010.
[17] A. Puc, G. Grosso, P. Gavrilovic, H. Fevrier, A. Kaminski, S. Burtsev, D. Chang, M. Foster, W. Pelouch, and P. Perrier, "Ultra-wideband10.7 Gb/s NRZ terrestrial transmission beyond 3000 km using all-Raman amplifiers," Proc. ECOC2005, paper Mo.3.2.5, Sept. 2005.
[18] H. Takara, H. Masuda, K. Mori, K. Sato, Y. Inoue, T. Ohara, A. Mori, M. Kohtoku, Y. Miyamoto, T. Morioka, and S. Kawanishi, "Ultra-wideband tellurite/silica fiber Raman amplifier and supercontinuum lightwave source for 124-nm seamless bandwidth DWDM transmission," Proc. OFC2002, paper FB1, March 2002.
[19] N. Kikuchi, "Intersymbol interference (ISI) suppression technique for optical binary and multilevel signal generation," J. Lightwave Technol., vol.25, no.8, pp.2060–2068, Aug. 2007.
[20] T. Sakamoto, A. Chiba, and T. Kawanishi, "50-Gb/s 16 QAM by a quad-parallel Mach-Zehnder modulator," Proc. ECOC2007, paper PD2.8, Sept. 2007.
[21] H. Yamazaki, T. Yamada, T. Goh, Y. Sakamaki, and A. Kaneko, "64QAM modulator with a hybrid configuration of silica PLCs and $LiNbO_3$ phase modulators for 100-Gb/s applications," Proc. ECOC2009, paper 2.2.1, Sept. 2009.
[22] A. Sano, T. Kobayashi, K. Ishihara, H. Masuda, S. Yamamoto, K. Mori, E. Yamazaki, E. Yoshida, Y. Miyamoto, T. Yamada, and H. Yamazaki, "240-Gb/s polarization-multiplexed 64-QAM modulation and blind detection using PLC-LN hybrid integrated modulator and digital coherent receiver," Proc. ECOC2009, paper PD2.2, Sept. 2009.
[23] T. Yamada, Y. Sakamaki, T. Shibata, A. Kaneko, A. Sano, and Y. Miyamoto, "Compact 111-Gbit/s integrated RZ-DQPSK modulator using hybrid assembly technique with silica-based PLCs and $LiNbO_3$ devices," Proc. OFC/NFOEC2008, paper OThC3, Feb. 2008.
[24] Y. Mori, C. Zhang, K. Igarashi, K. Katoh, and K. Kikuchi, "Phase-noise tolerance of optical 16-QAM signals demodulated with decision-directed carrier-phase estimation," Proc. OFC/NFOEC2009, paper OWG7, March 2009.
[25] H. Ishii, K. Kasaya, and H. Oohashi, "Spectral linewidth reduction in widely wavelength tunable DFB laser array," IEEE J. Sel. Top. Quantum Electron., vol.15, no.3, pp.514–520, May 2009.
[26] K. Nagayama, M. Kakui, M. Matsui, T. Saitoh, and Y. Chigusa, "Ultra-low-loss (0.1484 dB/km) pure silica core fiber and extension of transmission distance," Electron. Lett., vol.38, no.20, pp.1168–1169, Sept. 2002.
[27] H. Masuda, E. Yamazaki, A. Sano, T. Yoshimatsu, T. Kobayashi, E. Yoshida, Y. Miyamoto, S. Matsuoka, Y. Takatori, M. Mizoguchi, K. Okada, K. Hagimoto, T. Yamada, and S. Kamei, "13.5-Tb/s (135 × 111-Gb/s/ch) no-guard-interval coherent OFDM transmission over 6,248 km using SNR maximized second-order DRA in the extended L-band," Proc. OFC/NFOEC2009, paper PDPB5, March 2009.
[28] H. Masuda and Y. Miyamoto, "Low-noise extended L-band phosphorus co-doped silicate EDFA consisting of novel two-stage gain-flattened gain blocks," Electron. Lett., vol.44, no.18, pp.1082–1083, Aug. 2008.
[29] Y. Sakamaki, H. Yamazaki, T. Mizuno, T. Goh, Y. Nasu, T. Hashimoto, S. Kamei, K. Hattori, H. Takahashi, T. Kobayashi, and M. Ishikawa, "Dual polarization optical hybrid using silica-based planar lightwave circuit technology for digital coherent receiver," Electron. Lett., vol.46, no.1, pp.58–60, Jan. 2010.
[30] T. Kobayashi, A. Sano, H. Masuda, K. Ishihara, E. Yoshida, Y. Miyamoto, H. Yamazaki, and T. Yamada, "160-Gb/s polarization-multiplexed 16-QAM long-haul transmission over 3,123 km using digital coherent receiver with digital PLL based frequency offset compensator," Proc. OFC/NFOEC2010, paper OTuD1, March 2010.
[31] K. Ishihara, T. Kobayashi, R. Kudo, Y. Takatori, A. Sano, and Y. Miyamoto, "Frequency-domain equalization for coherent optical single-carrier transmission systems," IEICE Trans. Commun., vol.E92-B, no.12, pp.3736–3743, Dec. 2010.
[32] J. Yang, J.-J. Werner, and G.A. Dumont, "The multimodulus blind equalization and its generalized algorithms," IEEE J. Sel. Areas Commun., vol.20, no.5, pp.997–1015, June 2002.

[33] K.C. Hung and D.W. Lin, "Joint carrier recovery and multimodulus blind decision-feedback equalization under high-order QAM," Proc. Globecomm2004, pp.2281–2285, 2004.
[34] S.J. Savory, "Digital filters for coherent optical receivers," Opt. Express, vol.16, no.2, pp.804–817, 2008.
[35] G. Charlet, M. Salsi, P. Tran, M. Bertolini, H. Mardoyan, J. Renaudier, O. Bertran-Pardo, and S. Bigo, "72 × 100 Gb/s transmission over transoceanic distance, using large effective area fiber, hybrid Raman-Erbium amplification and coherent detection," Proc. OFC/NFOEC2009, paper PDPB6, March 2009.
[36] Y. Miyamoto, A. Hirano, K. Yonenaga, A. Sano, H. Toba, K. Murata, and O. Mitomi, "320 Gbit/s (8 × 40 Gbit/s) WDM transmission over 367 km with 120 km repeater spacing using carrier-suppressed return-to-zero format," Electron. Lett., vol.35, no.23, pp.2041–2042, Nov. 1999.
[37] M. Valkama, M. Renfors, and V. Koivunen, "Blind signal estimation in conjugate signal models with application to I/Q imbalance compensation," IEEE Signal Process. Lett., vol.12, no.11, pp.733–736, Nov. 2005.

Akihide Sano received the B.S. and M.S. degrees in physics and Ph.D. degree in communication engineering from Kyoto University, Kyoto, Japan, in 1990, 1992, and 2007, respectively. In 1992, he joined the NTT Transmission Systems Laboratories, Yokosuka, Kanagawa, Japan, where he was engaged in research and development on high-speed optical communication systems. His current research interests include large-capacity long-haul fiber-optic communication systems. He received the Best Paper Award of the First Optoelectronics and Communication Conference (OECC'96) in 1996, the Young Engineer Award in 1999, and the Achievement Award in 2010 from IEICE.

Takayuki Kobayashi received his B.E. and M.E. degrees in communications engineering from Waseda University, Tokyo, Japan, in 2004 and 2006, respectively. Since April 2006, he has been with NTT Network Innovation Laboratories, NTT, Yokosuka, Japan. His current research interests are modulation formats, coherent detection and high speed fiber-optic communications systems.

Eiji Yoshida received the B.S., M.S., and Ph.D. degrees in engineering physics from Kyoto University, Japan, in 1988, 1990, 2001, respectively. He joined Nippon Telegraph and Telephone (NTT) Corporation in 1990. He has been engaged in research on high-speed optical transport network and large-capacity optical communication system. He is now the senior research engineer, supervisor, of NTT Network Innovation Laboratories.

Yutaka Miyamoto received the B.E. degree and M.E. degree in electrical engineering from Waseda University, Tokyo, Japan, in 1986 and 1988, respectively. In 1988, he joined the NTT Transmission Systems Laboratories, Yokosuka, Japan, where he engaged in research and development on 10 Gbit/s optical communications systems. He is now the distinguished researcher and the group leader of NTT Network Innovation Laboratories. His current research interest includes high-capacity optical transport network with advanced modulation formats and digital signal processing. He is a member of the IEEE. He received the Achievement Award from IEICE in 2010.